Data in Brief 4 (2015) 577–582

Contents lists available at ScienceDirect

Data in Brief

journal homepage: www.elsevier.com/locate/dib

Data Article

A probabilistic atlas of the basal ganglia using 7 T MRI

Max C. Keuken, Birte U. Forstmann *

Amsterdam Brain and Cognition, University of Amsterdam, Nieuwe Prinsengracht 130, 1018VZ Amsterdam, The Netherlands

ARTICLE INFO

Article history:
Received 9 June 2015
Received in revised form
8 July 2015
Accepted 13 July 2015
Available online 31 July 2015

Keywords:
Basal ganglia
Probabilistic atlas
7 T MRI

ABSTRACT

A common localization procedure in functional imaging studies includes the overlay of statistical parametric functional magnetic resonance imaging (fMRI) maps or coordinates with neuroanatomical atlases in standard space, e.g., MNI-space. This procedure allows the identification of specific brain regions. Most standard MRI software packages include a wide range of atlases but have a poor coverage of the subcortex. We estimated that approximately 7% of the known subcortical structures are mapped in standard MRI-compatible atlases [1]. Here we provide a data description of a subcortical probabilistic atlas based on ultra-high resolution in-vivo anatomical imaging using 7 T (T) MRI. The atlas includes six subcortical nuclei: the striatum (STR), the globus pallidus internal and external segment (GPi/e), the subthalamic nucleus (STN), the substantia nigra (SN), and the red nucleus (RN). These probabilistic atlases are shared on freely available platforms such as NITRC and NeuroVault and are published in NeuroImage "Quantifying inter-individual anatomical variability in the subcortex using 7 T structural MRI" [2].

* Corresponding author.
E-mail address: buforstmann@gmail.com (B.U. Forstmann).

http://dx.doi.org/10.1016/j.dib.2015.07.028

Specifications table

Subject area	Psychology
More specific subject area	Cognitive neuroscience
Type of data	NifTI
How data was acquired	7 T magnetic resonance imaging
Data format	Analyzed
Experimental factors	Manual segmentations of six subcortical structures in young, healthy participants
Experimental features	The data was registered from individual to standard MNI-space using linear and non-linear registration algorithms creating a probabilistic atlas of six subcortical structures.
Data source location	Leipzig, Germany
Data accessibility	The data is located in two public repositories:http://neurovault.org/collections/550/https://www.nitrc.org/projects/atag/

1. Value of the data

1) Current brain atlases lack detailed information about subcortical brain structures.
2) Probabilistic atlas maps of six subcortical nuclei using ultra-high resolution 7 T MRI are included.
3) The probabilistic atlas maps are freely available.

2. Data, experimental design, materials and methods

2.1. Participants

The probabilistic atlas is based on 30 participants (14 females) with a mean age of 24.2 (SD 2.4). All participants had normal or corrected-to-normal vision, and none of them had a history of neurological, major medical, or psychiatric disorders. All subjects were right-handed, as confirmed by the Edinburgh Inventory [3]. The study was approved by the local ethics committee at the University of Leipzig, Germany. All subjects gave their written informed consent prior to scanning and received a monetary compensation for participating.

2.2. Scan parameters

The structural data were acquired using a 7 T (T) Siemens Magnetom MRI scanner with a 24-channel head array Nova coil (NOVA Medical Inc., Wilmington MA) and consisted of three MRI sequences: a whole-brain T_1-weighted MP2RAGE, a zoomed T_1-weighted MP2RAGE [4,5], and a zoomed multi-echo 3D T_2^*-weighted FLASH [6]. The whole-brain MP2RAGE had 240 sagittal slices with an acquisition time of 10:57 min (repetition time (TR)=5000 ms; echo time (TE)=2.45 ms; inversion times TI1/TI2=900/2750 ms; flip angle=5°/3°; bandwidth=250 Hz/Px; voxel size=0.7 mm^3). The MP2RAGE slab consisted of 128 slices with an acquisition time of 9:07 min (TR=5000 ms; TE=3.71 ms; TI1/TI2=900/2750 ms; flip angle=5°/3°; bandwidth=240 Hz/Px; voxel size=0.6 mm^3). The FLASH slab consisted of 128 slices with an acquisition time of 17:18 min (TR=41 ms and three different echo times (TE)=11.22/20.39/29.57 ms; flip angle=14°; bandwidth=160 Hz/Px; voxel size=0.5 mm^3). The slab sequences consisted of axial slices tilted to the orientation of the AC-PC line. Quantitative susceptibility maps (QSM) were calculated using the phase information of the FLASH MRI sequence and the method proposed by Schweser et al.[7]; see Ref. [8]

for more information about the exact scan protocols. The MP2RAGE and FLASH scans are freely available on www.nitrc.org/projects/atag_mri_scans/ or http://datadryad.org/resource/http://dx.doi.org/10.5061/dryad.fb41s

2.3. Scan sequence and region of interest

The visibility of each structure varied across the three different scan contrasts. The striatum (STR) was best visible in the T_1-weighted MP2RAGE 0.6 mm isotropic slab sequence whereas the T_2^*-weighted FLASH 0.5 mm isotropic slab sequences was used to segment the subthalamic nucleus (STN), substantia nigra (SN), and red nucleus (RN). Finally the globus pallidus externa (GPe) and interna (GPi) were segmented on the QSM 0.5 mm isotropic maps.

2.4. Segmentation protocol

Manual segmentation was carried out by two independent researchers using the FSL 4.1.4 viewer (http://fsl.fmrib.ox.ac.uk/fsl/fslwiki/). Only voxels rated by both raters as belonging to a particular structure were included in the probabilistic atlas. The manual segmentation was done as follows: in an initial step, the MRI volume was loaded into the viewer separately for each participant. Second, the contrast values in the viewer for the image were set to increase the visibility of the structural boarders. The contrast values were determined on an individual subject basis, separate for each structure, and were independently set by each rater. The contrast values were kept constant between hemispheres. Third, either the coronal, sagittal, or transverse view was randomly picked to start delineating the structure. Once the delineation of the structure started, all three the views were used to segment the structure. The order in which the right or left hemisphere was segmented was randomized per participant. Finally, per structure, the inter-rater reliability (Cohen's kappa, Dice coefficient, and intra-class correlation coefficient (ICC)) was calculated [9–11]. The mean Cohen's kappa ranged between 0.76 and 0.89 across structures. The mean Dice coefficient ranged between 0.72 and 0.89, and the ICC ranged between 0.72 and 0.87 across structures, indicating that all probabilistic maps have good inter-rater agreement. See [2] for the Cohen's kappa, Dice, and ICC for each individual structure.

2.5. Registration to standard stereotactic MNI space

All linear registration steps were done using MIPAV 5.4.4. (http://mipav.cit.nih.gov/) using the optimized automated linear registration algorithm. The MP2RAGE scans were skull stripped using the MP2RAGE skull strip algorithm as implemented in the CBS High-Res Brain Processing Tools for MIPAV (http://www.cbs.mpg.de/institute/software/cbs-hrt/index.html). The FLASH scans were skull stripped using BET as implemented in FSL (http://fsl.fmrib.ox.ac.uk/fsl/). The whole-brain MP2RAGE was linearly registered to the MNI04 template using a correlation ratio and 12° of freedom (DOF). The MNI04 template is included the CBS toolbox and is a copy of the non-linear 6th generation MNI ICBM152 template [12,13], but resampled at a 0.4 mm isotropic resolution. The MP2RAGE slab was then linear registered to the MP2RAGE whole brain in MNI space using a correlation ratio and 12 DOF. The FLASH slab was registered to the MNI04 in several steps: first the FLASH slab was linear registered to the original MP2RAGE slab using a correlation ratio and 7 DOF. The FLASH slab was then transformed to the MNI04 space using the transformation matrix that was generated by the MP2RAGE slab to MP2RAGE whole brain in MNI-space registration.

The six subcortical maps were transformed to the MNI04 template using the transformation matrices that were either generated by the MP2RAGE slab to whole-brain MP2RAGE registration or by the two transformation matrices that were used for the FLASH to whole-brain MP2RAGE registration.

All registration steps were visually checked for misalignments by comparing several landmarks. The landmarks that were checked within each subject were the 4th ventricle, pons, corpus callosum, and lateral ventricles. The landmarks that were checked for each registration to MNI-space were the surface of the brain, corpus callosum, and lateral ventricles. For four participants, the MP2RAGE slab did not register correctly to the whole-brain MP2RAGE image. For these participants, the linear registration was repeated

but with a smaller rotation search step (instead of using steps of 30° for the initial coarse rotation, steps of 15° were used). All other registration steps and parameters were identical. Additionally, the linear registered whole-brain individual scans and the segmented structures in MNI04 space were non-linearly optimized using ANTS (https://github.com/stnava/ANTs). The non-linear optimization was based on the mutual information of the whole-brain MP2RAGE and the MNI04 template using a Gaussian regularization, nearest neighbor interpolation and 40 coarse, 50 medium, and 40 fine iterations [14,15]. Subsequently, all individual masks in MNI04 stereotactic space were added together to create a probabilistic atlas of each structure and hemisphere separately with a 0.4 mm isotropic resolution [2].

The atlas has four different versions: a linear, a non-linear, a normalized, and a non-normalized version. The linear and non-linear atlas versions were created by registering the individual maps, either linearly, or optimized non-linearly to MNI space, respectively. The non-normalized atlas has a probability range between 0.0 and 30.0. Dividing the non-normalized atlas by 30, which was the maximum number of participants that could overlap in a given voxel, created a normalized probability range between 0.0 and 1.0. Due to the use of trilinear interpolation, the probability values within the probabilistic atlases are not discrete. All four versions of the atlas can be found on http://neurovault.org/collections/550/ or https://www.nitrc.org/projects/atag/. Whether the linear or non-linear atlas should be used is dependent on the registration strategy on the user end. If the user only used linear registrations to MNI standard space, the corresponding linear atlas should be used.

In addition to the individual masks, a combined version of all masks is provided which has been thresholded to only include the overlapping voxels for at least 10 participants (see Fig. 1).

Fig. 2 The maximum percentage overlap across participants for each linearly registered structure in MNI space was high for the large structures (STR left: 100%, STR right: 100%, GPe left: 96.66%, GPe right: 96.66%, GPi left: 96.66%, GPi right: 96.66%, RN right: 100%, RN left: 100%). A substantial lower overlap was found for the smaller structures (SN left: 76.66%, SN right: 63.33%, STN left: 56.66, STN right: 53.33%). See Fig. 3 for the histograms indicating the overlap between participants per structure and hemisphere.

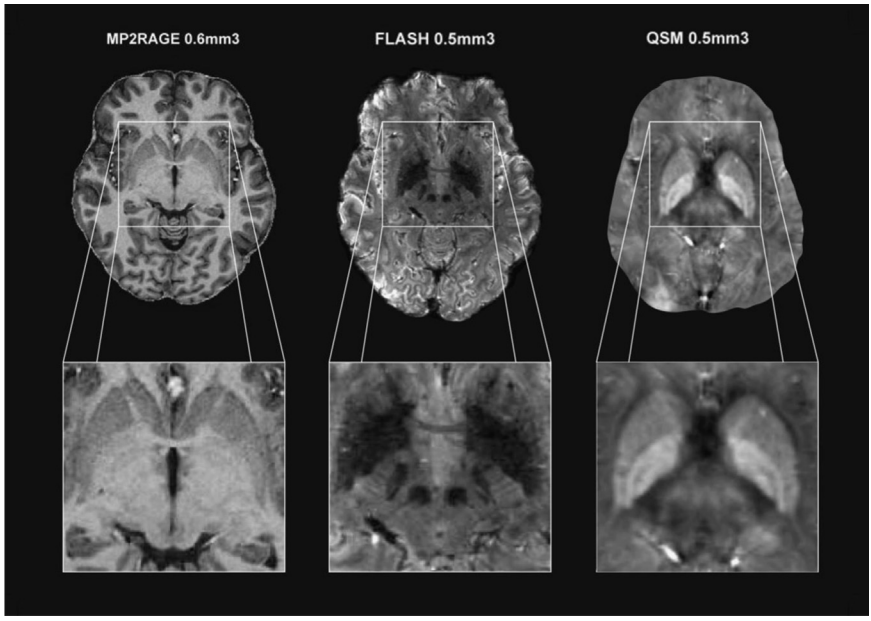

Fig. 1. MRI scan sequences used for creating probabilistic atlas maps. Left: T1-weighted MP2RAGE sequence; middle: T2*-weighted FLASH sequence; right: QSM. Reprinted from [2], with permission from Elsevier.

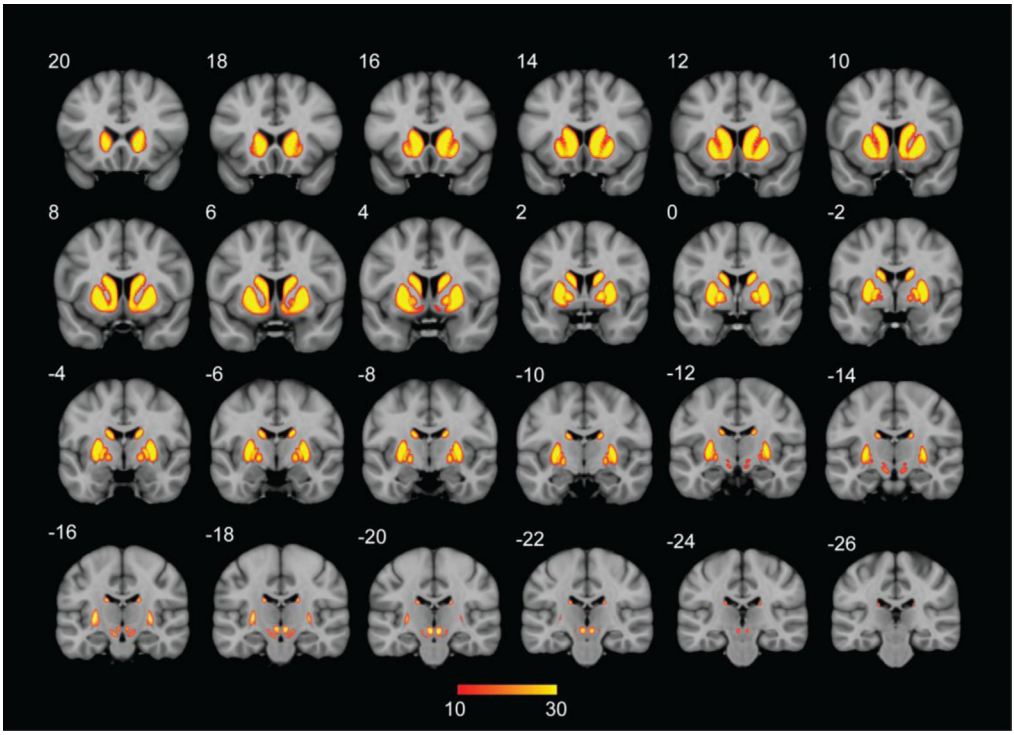

Fig. 2. The thresholded probability atlas of the striatum, the internal and external segment of the globus pallidum, subthalamic nucleus, substantia nigra, and red nucleus in standard MNI space. The numbers correspond to the *Y* coordinate. The colors indicate the overlap across the 30 participants with a minimum overlap of 10 participants.

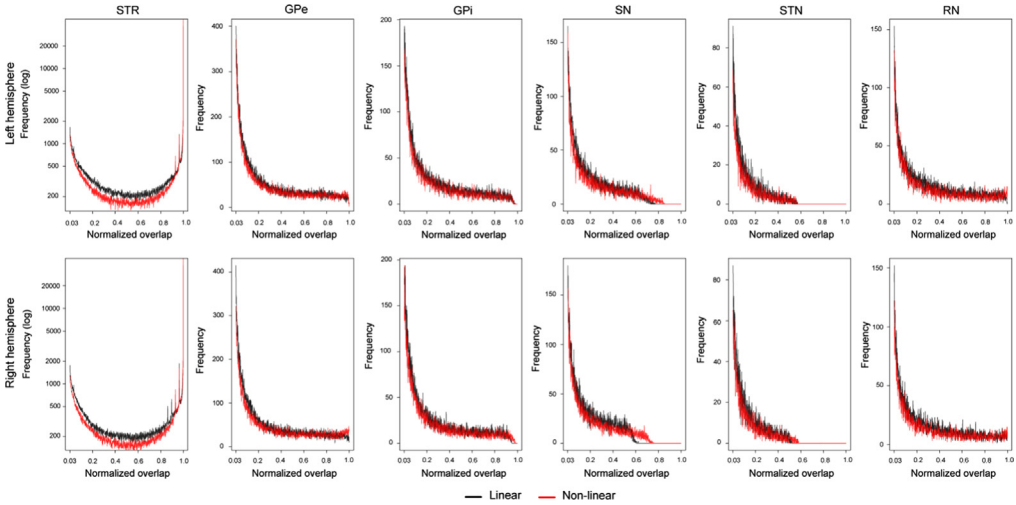

Fig. 3. The intensity histograms per structure and hemisphere. In black: the normalized overlap between participants per structure that were registered to MNI space using the linear registration. In red: the normalized overlap between participants per structure that were registered to MNI space using the non-linear registration.

2.6. Limitations

The atlas can be useful for most MRI studies within the cognitive neurosciences because it is based on healthy young participants [16,17]. However, users should be cautious applying this atlas to other age groups including elderly participants because of increased anatomical variability across the adult lifespan [17–23].

3. Conclusion

The current probabilistic atlas of the basal ganglia and red nucleus is a first step in mapping the human subcortex using structural 7 T MRI. Ongoing work is focused on manually segmenting additional structures and to incorporate middle-aged and elderly age groups.

References

[1] A. Alkemade, M.C. Keuken, B.U. Forstmann, A perspective on terra incognita: uncovering the neuroanatomy of the human subcortex, Front. Neuroanat. 7 (2013) 50, http://dx.doi.org/10.3389/fnana.2013.00040.
[2] M.C. Keuken, et al., Quantifying inter-individual anatomical variability in the subcortex using 7 T structural MRI, NeuroImage 94 (2014) 1–7.
[3] R.C. Oldfield, The assessment and analysis of handedness: the Edinburgh inventory, Neuropsychologia 9 (1971) 97–113.
[4] A.C. Hurley, A. Al-Radaideh, L. Bai, U. Aickelin, R. Coxon, P. Glover, P.A. Gowland, Tailored RF pulse for magnetization inversion at ultrahigh field, Magn. Reson. Med. 63 (1) (2010) 51–58, http://dx.doi.org/10.1002/mrm.22167.
[5] J.P. Marques, et al., MP2RAGE, a self bias-field corrected sequence for improved segmentation and T1-mapping at high field, NeuroImage 49 (2010) 1271–1281.
[6] A. Haase, J. Frahm, D. Matthaei, W. Hanicke, K.D. Merboldt, FLASH imaging. Rapid NMR imaging using low flip-angle pulses, J. Magne. Resonan. 67 (1986) 258–266.
[7] F. Schweser, A. Deistung, K. Sommer, J.R. Reichenbach, Toward online reconstruction of quantitative susceptibility maps: superfast dipole inversion, Magn. Resonan. Med. 69 (2012) 1581–1593.
[8] B.U. Forstmann, et al., Multi-modal ultra-high resolution structural 7-Tesla MRI data repository. Scientific Data 1 SP–EP-, 140050, 2014.
[9] J. Cohen, A coefficient of agreement for nominal scales, Educ. Psychol. Meas. 20 (1960) 37–46.
[10] L.R. Dice, Measures of the amount of ecologic association between species, Ecology 26 (1945) 297–302.
[11] P.E. Shrout, J.L. Fleiss, Intraclass correlations: uses in assessing rater reliability, Psychol. Bull. 86 (1979) 420.
[12] G. Grabner, A.L. Janke, M.M. Budge, D. Smith, J. Pruessner, D.L. Collins, Symmetric atlasing and model based segmentation: an application to the hippocampus in older adults. Medical Image Computing and Computer-Assisted Intervention – Miccai 2006, Pt 2, 4191, 58–66, 2006.
[13] V. Fonov, A.C. Evans, K. Botteron, C.R. Almli, R.C. McKinstry, D.L. Collins, T.B.D.C. Group, Unbiased average age-appropriate atlases for pediatric studies, NeuroImage 54 (1) (2011) 313–327, http://dx.doi.org/10.1016/j.neuroimage.2010.07.033.
[14] B. Avants, et al., Multivariate analysis of structural and diffusion imaging in traumatic brain injury, Acad. Radiol. 15 (2008) 1360–1375.
[15] B.B. Avants, et al., A reproducible evaluation of ANTs similarity metric performance in brain image registration, NeuroImage 54 (2011) 2033–2044.
[16] J.Y. Chiao, Cultural neuroscience: a once and future discipline, Prog. Brain Res. 178 (2009) 287–304.
[17] J. Henrich, S.J. Heine, A. Norenzayan, The weirdest people in the world? Behav. Brain Sci. 33 (2010) 61–83.
[18] A.W. Toga, P.M. Thompson, E.R. Sowell, Mapping brain maturation, Trends Neurosci. 29 (2006) 148–159.
[19] D.L. Greenberg, et al., Aging, gender, and the elderly adult brain: an examination of analytical strategies, Neurobiol. Aging 29 (2008) 290–302.
[20] A.C. Evans, A.L. Janke, D.L. Collins, S. Baillet, Brain templates and atlases, NeuroImage 62 (2012) 911–922.
[21] M.C. Keuken, et al., Ultra-high 7 T MRI of structural age-related changes of the subthalamic nucleus, J. Neurosci. 33 (2013) 4896–4900.
[22] W.F. Den Dunnen, M.J. Staal, Anatomical alterations of the subthalamic nucleus in relation to age: a postmortem study, Mov. Disord. 20 (2005) 893–898.
[23] M. Kitajima, et al., Human subthalamic nucleus: evaluation with high-resolution MR imaging at 3.0 T, Neuroradiology 50 (2008) 675–681.